University of East London Institutional Repository: http://roar.uel.ac.uk

This paper is made available online in accordance with publisher policies. Please scroll down to view the document itself. Please refer to the repository record for this item and our policy information available from the repository home page for further information.

EXTERNALLY CONFINED CONCRETECOLUMNS USING FRP TUBES

M.A. Ciupala, K. Pilakoutas, A.A. Mortazavi
University of East London, UK, University of Sheffield, UK,
Power and Water University of Technology, Tehran, Iran
m.a.ciupala@uel.ac.uk, k.pilakoutas@sheffield.ac.uk, mraa1350@gmail.com

Abstract: This paper presents an experimental investigation carried out on concrete filled fibre reinforced polymers (FRP) tubes, subjected to monotonic and cyclic loading. Two types of FRP materials were used: glass fibres and carbon fibres. Different failure modes and the effect of concrete fill, type of confinement materials, reinforcement ratio based on tube thickness and type of loading are examined. The study shows that external confinement of concrete by means of modern materials, such fibre reinforced polymers, can enhance its strength and ductility as well as result in large energy absorption capacity. This has important safety implications, especially in regions with seismic activity. A model that predicts the behaviour of confined concrete which takes into account the stiffness and effectiveness of different confinement materials is briefly introduced.

1. Introduction:

Retrofitting of concrete columns by wrapping using FRP materials has become a well-established technique which has been successfully used in the field, (Saadatmanesh, 1994).
Concrete-filled FRP tubes have been proposed as a practical solution for the construction of new concrete columns, (Mirmiran, 1995). The tube acts as a formwork, confinement, longitudinal and transverse reinforcement for the concrete core and protection against corrosion. Such FRP-concrete structures may overcome problems encountered with traditional concrete-filled steel tubes.
Research on concrete-filled FRP tubes has been limited to the study of their behaviour under monotonic loading, (Mirmiran, 1995), (Saafi, 1999) whilst a limited number of studies were carried out on concrete-filled FRP tubes under cyclic loading.

This paper presents details of experimental work carried out on concrete-filled FRP tubes subjected to both monotonic and cyclic loading. An extensive presentation of this experimental work is shown in (Mortazavi, 2002). This research was conducted at the Centre for Cement and Concrete of the University of Sheffield, UK. The research formed part of work undertaken under the EU TMR Network ConFibreCrete.

2. Experimental investigation:

2.1. Specimen details, instrumentation and test procedure:

Twelve concrete-filled FRP tubes were manufactured and tested. Two FRP materials (carbon fibres - CFRP and glass fibres - GFRP) were used for the construction of the FRP tubes. The mechanical properties of the fibres are shown in Table 1. Three tube thicknesses

were considered: 1,2,3 layers of CFRP material and 2,3,4 layers of GFRP material. The inside diameter of the tubes was 100 mm and the height was 200 mm.

Mechanical properties	CFRP	GFRP
Nominal thickness t_j (mm)	0.117	0.135
Young's modulus E_j (MPa)	240000	65000
Ultimate tensile strength f_u (MPa)	3900	1700
Ultimate elongation ε_u (%)	1.55	2.80

Table 1: Mechanical properties of fibres

Ready-mixed concrete was used to fill the FRP tubes. A total of 10 concrete cylinder control specimens with a diameter of 100 mm and a height of 200 mm were cast and cured under the same conditions as the concrete-filled FRP tubes. Based on the cylinder test results at the time of testing, the average concrete strength (f_{co}) was 30 MPa. All the specimens were instrumented with five 15 mm strain gauges: three strain gauges were attached circumferentially at mid-height of each specimen, 120° apart, to measure lateral strain and two strain gauges were attached vertically at mid-height, to measure axial strain. In addition to the strain gauges, two other devices using Linear Variable Differential Transformers (LVDT) and Linear Potentiometer Displacement Transducers (LPDT) were used to measure the lateral and axial strain, respectively.

The tests were carried out using a servo-controlled hydraulic actuator with a capacity of 1000 kN. The specimens were labelled as follows: CML-n, where C denotes concrete filled tube, M denotes the confinement material ("C" for carbon and "G" for glass),

L is the number of layers of the FRP tube and n represents the sample number.

Some of the specimens were tested under uniaxial monotonic compression loading and some of them were tested under uniaxial cyclic loading, as shown in Table 2.

Loading/ Specimens	Monotonic	Cyclic
CFRP	CC1-1, CC1-2 CC2-1, CC3-1	CC2-2 CC3-2
GFRP	CG2-1, CG2-2 CG3-1, CG4-1	CG3-2 CG4-2

Table 2: Testing program

The cyclic loading was carried out in a quasi-static manner. The rate of loading was around 100 kN/min.

2.2. Failure modes:

The failure of all the specimens confined with CFRP tubes was sudden and occurred in an explosive manner.

Almost all of the CFRP tubes failed at different locations and a small rupture in the tube induced complete failure of the specimen, as shown in Figure 1. In vast majority of cases, the top and bottom part of the samples remained undamaged and hence did not deteriorate during failure. In general, the specimens tested under cyclic load experienced more damage than those tested under monotonic load.

The specimens confined by GFRP tubes failed in an explosive manner, by pure tensile failure of the tube. Almost all GFRP tubes ruptured through vertical rupture of the fabric, as shown in Figure 2. The rupture line was positioned between 25 and 35 mm away from the line of overlap.

2.3. Stress-strain behaviour:

2.3.1. CFRP confinement. In the case of specimens CC1-1 and CC1-2, the ultimate strength increased by about 75% of that of the plain (unconfined) concrete, f_{co}. In both cases, the failure took place before the full mobilisation of CFRP tube, at a lateral strain of about $10000\,\mu\varepsilon$.

Figure 2: Failure of concrete-filled GFRP tubes

Specimens CC2-1 and CC2-2 appeared to have developed the full capacity of the CFRP tube and both of them showed an ultimate strength more than two and a half times that of the unconfined concrete strength. CC2-1 showed a more ductile behaviour than that of CC2-2 and this may be attributed to concrete damage during cyclic loading.
In the case of specimen CC3-1, failure occurred before the full mobilisation of the CFRP strength with lateral strain less than $10000\,\mu\varepsilon$, while the specimen CC3-2 was very close to developing the full capacity of the tube. Both specimens achieved a very high strength enhancement, nearly three times the strength of the unconfined concrete.
Figure 3 shows the normalised axial stress versus the lateral and axial strain for the CC3 specimens. The normalised axial stress is defined as the ratio of f_{cl}/f_{co}, where f_{cl} is the axial compressive strength of the confined concrete. The horizontal positive axis represents the axial strains whilst the negative axis corresponds to the lateral strains.

2.3.2. GFRP confinement. The ultimate strength of specimens CG2-1 and CG2-2 increased by 34% relative to that of unconfined concrete.
In both cases, the tube was activated after reaching a load corresponding to the unconfined concrete strength.
In the case of the specimens CG3-1 and CG3-2, the strength of the confined concrete increased by about 50% and 40%, respectively. Failure occurred at a very low lateral strain in the tube. In the monotonic test, the lateral strain was only $3000\,\mu\varepsilon$, which may be due to tube damage caused by the crushed concrete, while in the cyclic test the specimen failed at around $7000\,\mu\varepsilon$.
In the case of specimens CG4-1 and CG4-2, the strength of the confined concrete increased by about 65% and 60%, respectively. A better mobilisation of the GFRP tube was achieved in these specimens, with a lateral strain reaching around $18000\,\mu\varepsilon$, as shown in Figure 4.
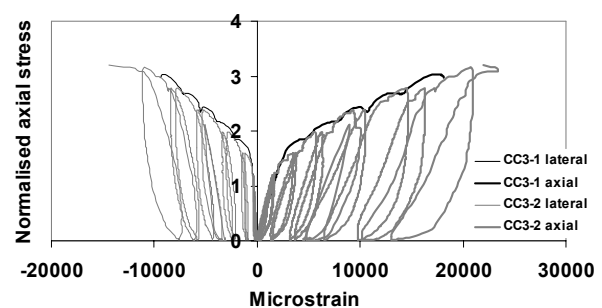

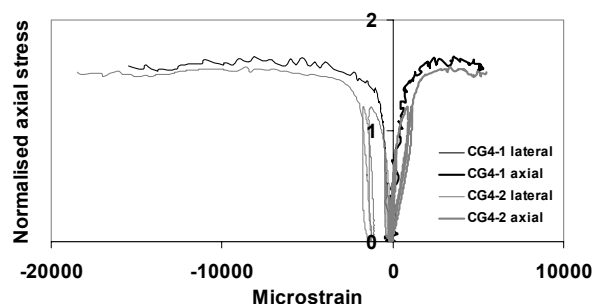Figure 3: Stress-strain curves for CC3 specimens

Figure 4: Stress-strain curves for CG4 specimens

2.4. Volumetric strain:

The normalised axial stress and normalised axial/lateral strain were plotted versus the volumetric strain. The normalised axial strain is expressed as $\varepsilon_{cl}/\varepsilon_{co}$ and the normalised lateral strain is defined as $\varepsilon_{cr}/\varepsilon_{cor}$, where ε_{cl} and ε_{cr} are the average axial and lateral strains in the confined concrete and ε_{co} and ε_{cor} are the average axial and lateral strains in the unconfined concrete ($\varepsilon_{co}=0.002$ and $\varepsilon_{cor}=0.001$). The volumetric strain is defined as $(V-V_o)/V_o$, where V_o and V are the initial and final volume of concrete, respectively.

2.4.1. CFRP confinement. Figure 5 shows the normalised axial stress versus the volumetric strain for specimens CC1-1 and CC1-2. The volumetric expansion of the concrete core started when the unconfined concrete strength f_{co} was reached. Even when the concrete starts to expand laterally due to the initiation of vertical cracking, the normalised axial stress is increasing up to failure. The relationship between the axial and lateral strain and the volumetric strain for CC1-1 and CC1-2 specimens is linear after the point of maximum contraction of the confined concrete, as shown in Figure 6.
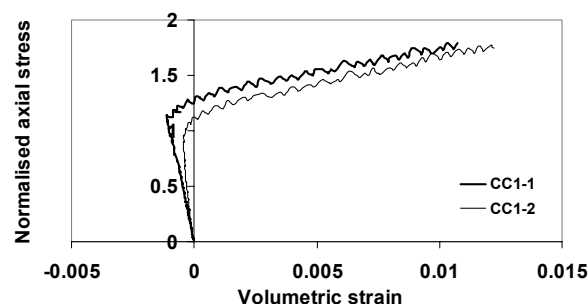

Figure 5: Normalised axial stress versus volumetric strain for CC1 specimens

In the case of the CC2-1 and CC2-2 specimens, the volumetric expansion of the concrete core also started after the stress f_{co} was reached, as shown in Figure 7.

CC2-2 specimen showed a more ductile behaviour than CC2-1. Once the expansion of the concrete takes place, the relationship between the lateral and axial strain and the volumetric strain is a quasi-linear one, as shown in Figure 8. The slope of the CC2-1 curve in Figure 8 is steeper than the one of CC2-2. This is likely to be due to the progressive damage of the concrete core during cyclic loading.

Sample CC3-1 exhibited volumetric contraction up to a stress of about $1.5 f_{co}$ and expanded only slightly before failure, as shown in Figure 9.

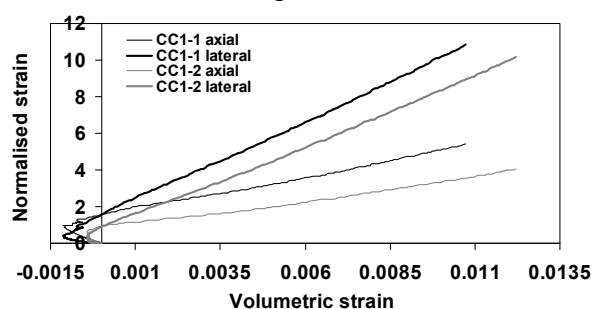Specimen CC3-2 showed no expansion at all and continued to compact until failure.

Figure 6: Normalised strain versus volumetric strain for CC1 specimens
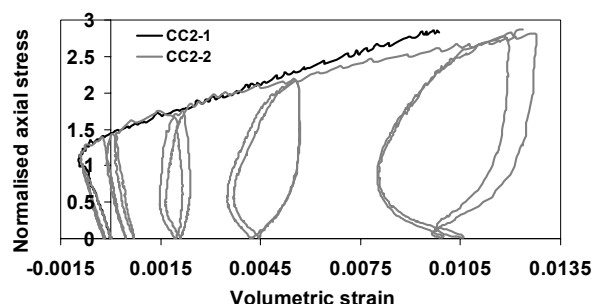
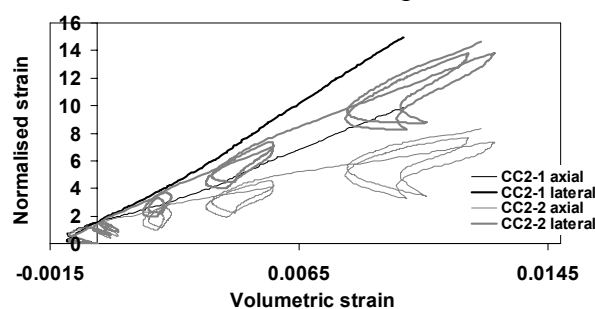Figure 7: Normalised axial stress versus volumetric strain for CC2 specimens

Figure 8: Normalised strain versus volumetric strain for CC2 specimens
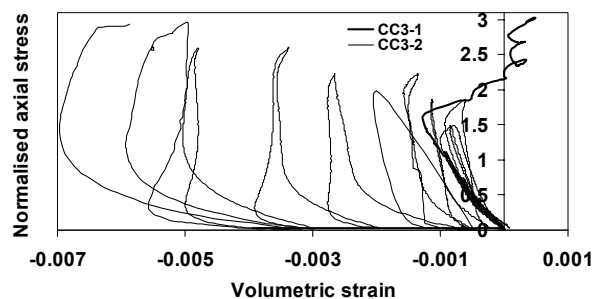

Figure 9: Normalised axial stress versus volumetric strain for CC3 specimens

This may be due to the fact that a large amount of lateral confinement was applied and concrete may have started to crush within the tube. However, this effect may also be attributed to the local effects around the strain gauges.

2.4.2. GFRP confinement. The volumetric expansion of CG2-1 and CG2-2 started at about 85% of the unconfined concrete strength, as noted in Figure 10.
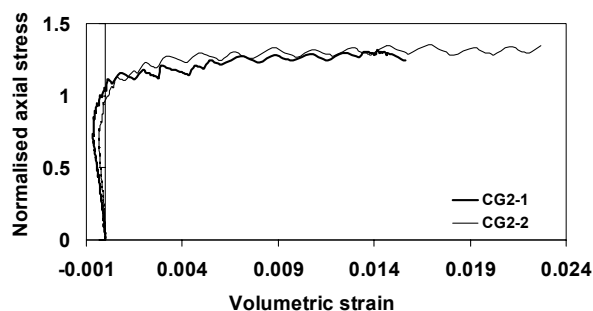

Figure 10: Normalised axial stress versus volumetric strain for CG2 specimens

The relationship between the axial and lateral strain and the volumetric strain is linear after the beginning of the expansion, as shown in Figure 11.

In the case of both CG3-1 and CG3-2, the contraction of the concrete core stopped at about $0.5 f_{co}$ and $0.4 f_{co}$, respectively, as shown in Figure 12. The subsequent volumetric expansion of CG3-1 also stopped at a very early stage, possibly due to the premature failure due to local damage of the fibres by the crushed concrete.

Figure 13 shows the linear variation between the axial and lateral strain and the volumetric strain for specimens CG3-1 and CG3-2.

In the case of samples CG4-1 and CG4-2, the expansion of concrete core started at about $0.5 f_{co}$ and $0.2 f_{co}$, respectively. The normalised strain in the axial and lateral direction versus the volumetric strain is shown in Figure 14.
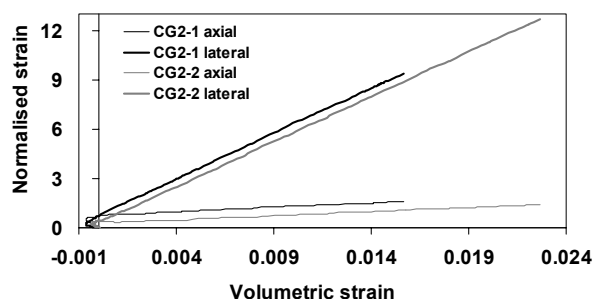

Figure 11: Normalised strain versus volumetric strain for CG2 specimens
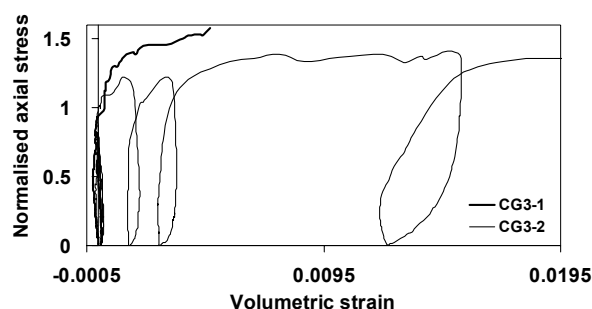
Figure 12: Normalised axial stress versus volumetric strain for CG3 specimens
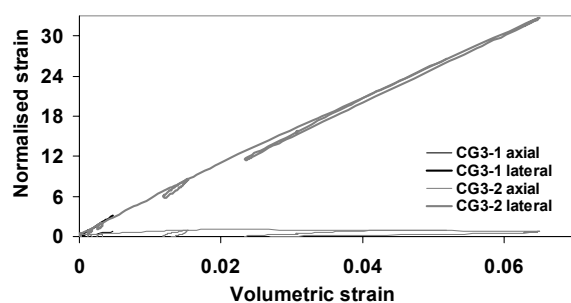

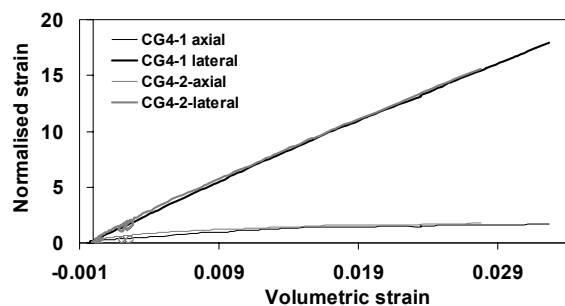Figure 13: Normalised strain versus volumetric strain for CG3 specimens

Figure 14: Normalised strain versus volumetric strain for CG4 specimens

Both samples exhibited a similar slope for the normalised axial and lateral strain and more or less a linear relationship between the normalised strain and the volumetric strain.

2.5. Discussion of the experimental results:

The results of the experimental work are summarised in Figures 15 and 16.

In these figures, the normalised ultimate axial stress f_{ccl}/f_{co} and normalised ultimate axial strain $\varepsilon_{ccl}/\varepsilon_{co}$ are plotted versus the effective confinement index $\alpha\omega_w$ (f_{ccl} and ε_{ccl} are the ultimate axial strength and ultimate axial strain, respectively, of the confined concrete). The coefficient $\alpha=1$ for circular sections and $\omega_w=2f_l/f_{co}$, where f_l is the confinement pressure exerted by the confinement material on the concrete core.

For all the confinement materials, an enhancement of the concrete strength is noted for both the monotonic and cyclic loading. The smallest increase in strength was achieved by the concrete-filled GFRP tubes, followed by the concrete-filled CFRP tubes.

In the case of concrete confined with CFRP tubes, an increase of 4% in strength was achieved under cyclic loading compared to the monotonic loading. For the concrete-filled GFRP tubes, the concrete strength under cyclic loading was around 7% less than the strength obtained under monotonic loading.

The stress-strain response of all specimens under cyclic loading is nonlinear, with a parabolic variation, up to failure.
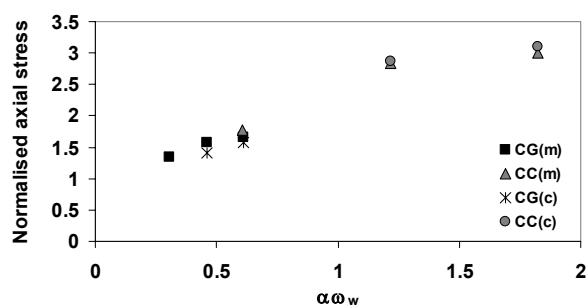

Figure 15: Normalised ultimate axial stress versus effective confinement index (m - monotonic; c - cyclic)
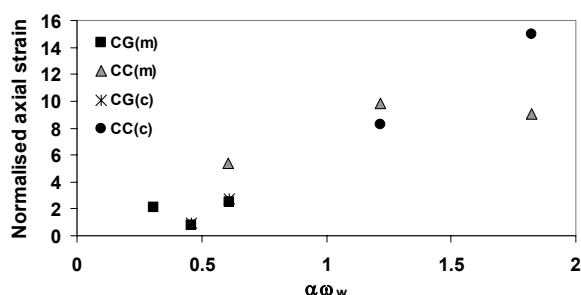
Figure 16: Normalised ultimate axial strain
versus effective confinement index
(m - monotonic; c - cyclic)

Energy dissipation during the unloading and reloading cycles is considerable in the case of the concrete-filled CFRP tubes, as shown in Figure 3. Significant plastic strains after unloading are also noticeable. No stiffness degradation upon reloading was observed.

In the case of the concrete-filled GFRP tubes, the energy dissipation and plastic strains were much lower than those obtained for the concrete confined with CFRP tubes. For all the confinement materials, the stress-strain relationship for the monotonic loading may serve as an envelope for cyclic loading. As shown in Figure 16, the normalised ultimate axial strains follow the same pattern as the normalised ultimate axial stresses presented in Figure 15. The smallest ultimate normalised axial strain was experienced by the concrete-filled GFRP tubes, followed by the concrete-filled CFRP tubes.

The relationship between the normalised axial strain and the volumetric strain for all the specimens is linear or quasi-linear. In the case of the concrete-filled FRP tubes, the normalised lateral strain increases with the increase of the number of FRP layers.

3. Analytical model:

An analytical model that predicts the behaviour of the confined concrete which takes into account the stiffness and effectiveness of the CFRP, GFRP and steel confinement was proposed by the authors, (Mortazavi, 2002). The model considers the varying pressure of the confinement on the concrete core. The confining strain and stress are determined through an incremental-iterative approach that generates the stress-strain diagram.

The ultimate axial strength f_{ccl} and the ultimate axial strain ε_{ccl} of the confined concrete are calculated using the following equations:

$$f_{ccl} / f_{co} = 1 + 1.7 \times {\alpha'\omega_w}^{0.8} \qquad (1)$$

$$\varepsilon_{ccl} / \varepsilon_{co} = \left[1 + 6.7 \left(f_{ccl} / f_{co} - 1 \right)^{\frac{2}{3}} \right] \qquad (2)$$

where $\alpha'\omega_w$ is the modified effective confinement index, which is calculated using the expression:

$$\alpha'\omega_w = 2 K_j \varepsilon_j / f_{co} \qquad (3)$$

The stiffness of the confinement K_j is defined as:

$$K_j = t_j E_j / D \qquad (4)$$

The lateral strain in the confining tube ε_j is calculated through an incremental-iterative approach.

Figure 17 shows the normalised ultimate axial stress f_{ccl} / f_{co} versus the modified effective confinement index $\alpha'\omega_w$. These results are compared with the ones obtained from the experiments.
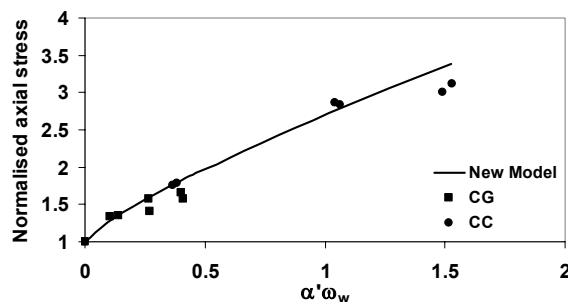
Figure 17: Normalised ultimate axial stress versus the modified effective confinement index $\alpha'\omega_w$

From Figure 17 it can be noted that the model predicts well the behaviour of the concrete-filled FRP tubes against the experimental results.

4. Conclusions:

The study shows that concrete confined with both FRP tubes has strength and deformability. Under monotonic loading, the FRP materials exhibit a bi-linear relationship between strain and stress, while under cyclic loading, this relationship becomes non-linear.

Depending on the stiffness and strength of the confining material, both the ductility and the concrete strength could increase under cyclic loading. This has important safety implications, especially in regions with seismic activity.

An analytical model that predicts the behaviour of the confined concrete which takes into account the stiffness and effectiveness of the CFRP and GFRP tubes is presented. The model predicts well the behaviour of the concrete-filled FRP tubes. Further work needs to be done in order to compare the results predicted by this model with the ones predicted by other models and/or obtained from experimental testing carried out by other authors.

5. References:

Mirmiran A., Shahawy M., "A novel FRP-concrete composite construction for the infrastructure", Proceedings Structural Congress XIII, ASCE, Boston, 1995, pp. 1663-1666.

Mortazavi A.A., *Behaviour of concrete confined with lateral pre-tensioned FRP*, PhD Thesis, The University of Sheffield, UK, 2002.

Saadatmanesh H., Ehsani M.R., Li M.W., "Strength and ductility of concrete columns externally reinforced with fibre composite straps", *ACI Structural Journal*, Vol. 91, No. 4, 1994, pp. 343-447.

Saafi M., Toutanji H.A., Li Z., "Behaviour of concrete columns confined with fibre reinforced polymer tubes", *ACI Structural Journal*, Vol. 96, No. 4, 1999, pp. 500-509.